

# In-Field Transport Properties at Grain Boundaries in BaHfO<sub>3</sub>-doped SmBa<sub>2</sub>Cu<sub>3</sub>O<sub>y</sub> Bicrystal Films at Low Temperatures

Y. Tsuchiya, J. Akita, Y. Ichino, S. Miura, and Y. Yoshida

**Abstract**—High-temperature superconducting REBCO tapes are attractive for their high critical current density  $J_c$  in magnetic fields. However,  $J_c$  in the REBCO film is suppressed under magnetic fields and by grain boundaries. Our group has reported that artificial pinning centers (APC) enhances the  $J_c$  at the grain boundaries in the REBCO films at the liquid nitrogen temperature of 77 K. In this study, we extended our previous work to a lower temperature since the usage of the REBCO tapes at a lower temperature and a high magnetic field is a recent development trend. Transport characteristics at grain boundaries in the REBCO films with and without APC were investigated at temperatures down to 4.2 K and at magnetic fields up to 9 T. The results show that the introduction of the APCs is effective to enhance the  $J_c$  at the grain boundaries at low temperatures and at the magnetic fields especially around the matching field where the density of the APC is equal to that of vortices.

**Index Terms**—Critical current, Grain boundaries, Coated conductors, Cuprates

## I. INTRODUCTION

THE high-temperature superconducting REBa<sub>2</sub>Cu<sub>3</sub>O<sub>y</sub> ( $RE =$  rare earth elements, REBCO) coated conductors is one of the promising conductors for application with superconducting magnets such as scientific high field magnets [1] or dipole magnets for accelerators [2]. For the magnet application, the critical current density  $J_c$  under a magnetic field needs to be improved. The keys to improve in-field  $J_c$  in the REBCO tapes are as follows: enhanced flux pinning using artificial pinning centers (APC) [3] and biaxial orientation using a buffer layer [4].

A number of researches on the APC in the REBCO films have been reported so far [5]-[10]. Non-superconducting perovskite oxide BaMO<sub>3</sub> ( $M$ : metal elements, BMO) is chemically stable in the REBCO matrix and grows like a rod by self-organized growth [5]. Since the BMO rod has good matching with the vortex core, the in-field  $J_c$  in the REBCO film is largely enhanced [6]. The metal elements such as Zr, Sn, and Hf have been reported as the  $M$  in the BMOs forming nanorods [6]-[8]. The BaHfO<sub>3</sub> (BHO) nanorod is one the most effective APC to

enhance the in-field  $J_c$ . Our group has reported the high flux pinning force density  $F_p$  in BHO-doped SmBa<sub>2</sub>Cu<sub>3</sub>O<sub>y</sub> (SmBCO) films as 1.5 TN/m<sup>3</sup> at 4.2 K and 21 T [9] and 32.5 GN/m<sup>3</sup> at 77 K and 5 T [10].

A grain boundary (GB) is another key factor to determine the  $J_c$  in the REBCO films [11]-[18]. The REBCO tape are biaxially oriented because the  $J_c$  at the GBs ( $J_c^{\text{GB}}$ ) exponentially decreases compared with in-grain  $J_c$  when a misorientation angle increases [11]-[14]. The  $J_c^{\text{GB}}$  starts to decrease at a critical misorientation angle ( $\theta_c$ ) [15]. On the other hand, several kinds of research revealed that the  $J_c^{\text{GB}}$  is equal to the in-grain  $J_c$  at high magnetic fields at 77 K [16]-[18]. To enhance in-field  $J_c^{\text{GB}}$ , it is necessary to improve the flux pinning of an Abrikosov-Josephson (A-J) vortex with an anisotropic core [19].

It is practically interesting whether the introduction of the APCs improves the in-field  $J_c^{\text{GB}}$  in REBCO films. So far, the  $J_c^{\text{GB}}$  characteristics in the REBCO films with the APCs has been reported only at 77 K [20], [21]. However, little is known about the in-field  $J_c^{\text{GB}}$  at low temperatures. In this study, the  $J_c^{\text{GB}}$  characteristics in REBCO films with and without the nanorod APCs are investigated at low temperature down to 4.2 K and high fields up to 9 T.

## II. EXPERIMENTAL METHOD

Undoped and BHO-doped SmBCO films were prepared by using the pulse laser deposition. The fabrication method is similar to our earlier report [21]. The films were fabricated with a KrF excimer laser ( $\lambda = 248$  nm), at 10 Hz repetition rate, with an energy density of 1.0 J/cm<sup>2</sup>, at an O<sub>2</sub> partial pressure of 400 mTorr, and at a substrate temperature of 870 °C. All the films had a thickness of 120 nm. BHO was doped into the films using the alternating-targets technique [22]. The BHO-doped films have content of BHO of 4.5vol.% which was determined by the inductively coupled plasma mass spectroscopy. The films were fabricated on (001) (LaAlO<sub>3</sub>)<sub>0.3</sub>-(SrAl<sub>0.5</sub>Ta<sub>0.5</sub>O<sub>3</sub>)<sub>0.7</sub>

Manuscript receipt and acceptance dates will be inserted here. Acknowledgment of support is placed in this paragraph as well. Consult the IEEE *Editorial Style Manual* for examples. This work was supported by the IEEE Council on Superconductivity under contract. ABCD-123456789. (*Corresponding author: Lance Cooley.*)

Y. Tsuchiya, J. Akita, Y. Ichino, Y. Yoshida is with the Department of Electrical Engineering, Nagoya University, Aichi, 464-8603, Japan (e-mail: tsuchiya@nuee.nagoya-u.ac.jp)

S. Miura is with the Institute of Superconductor Systems, Kyushu University, Fukuoka 819-0395, Japan

This research was partly supported by JST ALCA, JSPS KAKENHI Grant Numbers 15K14301, 15K14302, 15H04252, 16K20898.

Digital Object Identifier will be inserted here upon acceptance.

TABLE I  
SUPERCONDUCTING PROPERTIES OF THE FILMS.

Undoped/ BHO-doped	Misorientation Angle [°]	$T_c$ [K]	$J_c$ (77 K, self-field) [A/cm <sup>2</sup> ]
Undoped	0 (single crystal)	92.3	5.46
	5	91.8	2.45
	10	91.7	0.20
	15	92.2	0.08
BHO-doped	0 (single crystal)	90.6	2.69
	5	90.7	2.01
	10	90.5	0.29
	15	90.0	0.14

(LSAT) single crystal substrates and [001]-tilted bicrystal LSAT substrates with misorientation angles  $\theta$  of 5°, 10°, and 15°. The films were processed into micro-bridges including the GBs with a width of 50  $\mu\text{m}$  and a length of 1 mm by using the laser etching technique.

The current-voltage characteristics of the films were measured under a magnetic field  $B$  of 0 to 9 T and at a temperature  $T$  of 4.2 to 77 K by using PPMS (Quantum Design) and the four-probe method. During the measurement, the magnetic field was applied parallel to the  $c$ -axis of SmBCO which includes the GB plane. Applied current flowed perpendicular to the GBs. The non-ohmic linear differential region in which a voltage is not proportional but linearly different was observed for the films with  $\theta > 0^\circ$ .  $J_c$  was determined with an electric field criterion of 1 and 10  $\mu\text{V}/\text{cm}$  for the single crystal and the bicrystalline films, respectively.  $T_c$  was determined from the temperature-dependent resistivity with a criterion of 0.1  $\mu\Omega \cdot \text{cm}$ .

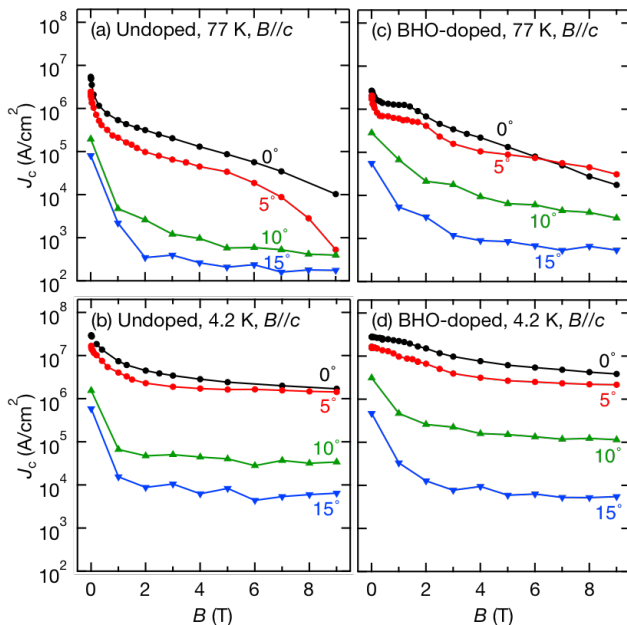


Fig. 1. Field dependence of  $J_c$  at grain boundary in the undoped and the BHO-doped SmBCO films at 77 K and 4.2 K.

### III. RESULTS AND DISCUSSION

#### A. Specification of films

Out-of-plane X-ray diffraction (XRD) showed diffraction peaks of (00 $l$ ) ( $l = 1, 2, 3, 4, 5, 6, 7, 8,$  and 9) SmBCO for all the fabricated films and an additional peak of (200) BHO only for the BHO-doped films. In-plane XRD for the bicrystalline films showed 2 strong diffraction peaks of (102) SmBCO whose difference was equal to the misorientation angle of the bicrystalline substrates. The result indicates the existence of the GB with a misorientation angle of  $\theta$ . Similar results were obtained for the BHO-doped films.

Tab. 1 shows the  $T_c$  and the  $J_c$  at 77 K and a self-field in the undoped and the BHO-doped SmBCO films. The  $T_c$ s in the BHO-doped films are slightly degraded by the BHO doping. On the other hand, the  $J_c$  drastically decreases by one order of magnitude or more for  $\theta > 5^\circ$ .

#### B. In-field flux pinning properties

Fig. 1 shows field dependences of the  $J_c$ s in the undoped and the BHO-doped films with  $\theta = 0-15^\circ$  at  $T = 4.2, 77$  K, and at  $B = 0-9$  T. When  $\theta = 0^\circ$ , it represents the film grown on a single crystal substrate. The  $J_c$  decreases with increasing  $\theta$  at all fields for both the undoped and the BHO-doped films as reported in earlier studies [21]. The  $J_c$  drastically drops at  $\theta$  between  $5^\circ$  and  $10^\circ$ , which indicates the transition from a low-angle GB to a high-angle GB. The in-field  $J_c$  in the BHO-doped films were larger than that in the undoped films, suggesting that the  $J_c^{\text{GB}}$  was improved by the BHO doping into the SmBCO films. The BHO-doped films with  $\theta = 0^\circ$  and  $5^\circ$  showed plateaus of  $J_c$  at  $B = 0.5-2$  T at 77 K. Let us compare the results of the transport characteristics with our previous results [21]. The field dependence of the  $J_c$  measured at 77 K is similar to that reported in our

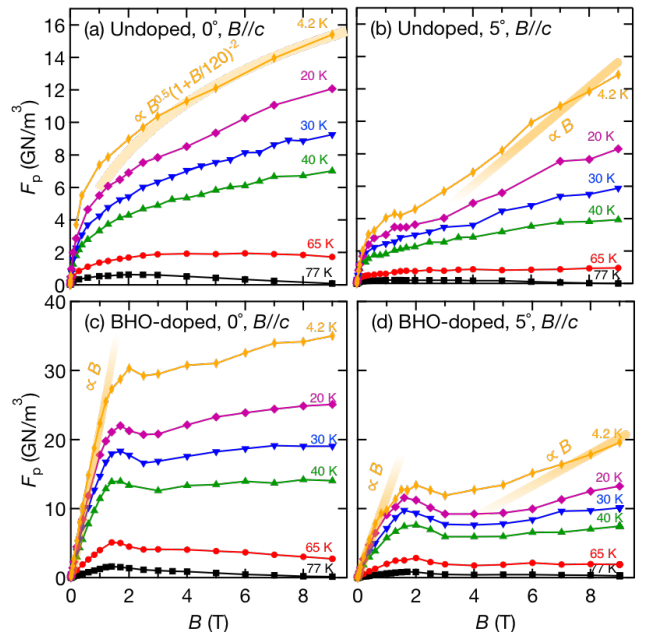


Fig. 2. Field dependence of  $F_p$  at grain boundary in (a, b) the undoped and (c, d) the BHO-doped SmBCO films with  $\theta =$  (a, c)  $0^\circ$ , (b, d)  $5^\circ$  at  $T = 4.2-77$  K.

previous study in terms of the plateau of the in-field  $J_c^{\text{GB}}$ . The plateaus of the  $J_c$  can be ascribed to the existence of  $c$ -axis oriented APCs in the films. In fact, according to the previous study, the transmission electron micrography clarified that the BHO-doped film had the BHO nanorod APCs which grew parallel to the  $c$ -axis of SmBCO in the grains and also at the GBs. Therefore, the similar field dependence of the  $J_c$  indicates that the BHO nanorods APCs are most likely grown in the films for this study. Turning now to the  $J_c$  properties at a low temperature, the  $J_c$  at 4.2 K is enhanced by the addition of BHO for  $\theta = 0^\circ$ ,  $5^\circ$ , and  $15^\circ$  as shown in Fig. 1(b) and (d). For example, the  $J_c^{\text{GB}}$  for  $\theta = 5^\circ$  was enhanced 1.5 times by the doping of the BHO APC. This result revealed that the introduction of the APC is effective to improve the  $J_c^{\text{GB}}$  even at a temperature less than 77 K. As a result different from the high temperature, the plateaus of the  $J_c$ s became less obvious. In the followings, we focus on the  $J_c$  properties for  $\theta = 0^\circ$  and  $5^\circ$  including the temperature dependence to discuss the origin of the enhanced flux pinning properties by the BHO doping.

Fig. 2 shows field dependences of the macroscopic flux pinning force densities  $F_p$ s ( $= J_c \times B$ ) in the undoped and the BHO-doped SmBCO films with  $\theta = 0^\circ$ ,  $5^\circ$  at various temperatures ranging from 4.2 to 77 K. As shown in Fig. 2(a), the  $F_p$  in the undoped film with  $\theta = 0^\circ$  has upward convex curves for all the temperatures. To clarify the origin of the flux pinning for the in-grain  $J_c$  in the undoped film, the field dependence of  $F_p$  is calculated based on the collective vortex pinning model and is shown as the orange curve in Fig. 2(a) [23]. Here, the typical field dependence of  $F_p$  as  $F_p(B) \propto B^{0.5}(1 - B/120)^2$  was assumed [9]. The field dependence of the  $F_p$  at a low temperature such as 4.2 K and at  $B > 4$  T follows the calculated line, which indicates that the in-grain  $J_c$  in the undoped SmBCO film with  $\theta = 0^\circ$  is explained with the collective flux pinning by the random flux pinning centers.

Next, as shown in Fig. 2(b), linear field dependences of the  $F_p$  at  $B > 2$  T are observed in the undoped SmBCO film with  $\theta = 5^\circ$ , which is obviously different from the upward convex field dependence for the in-grain flux pinning. For comparison, an orange straight line proportional to the magnetic field is drawn in Fig. 2(b). The linear field dependence of the  $F_p$  is explained by the correlated flux pinning model [23]. Diaz has reported that the A-J vortex at the GB is pinned by the dislocation in the bicrystalline YBCO film [24]. Therefore, the dislocation at the GB is a possible origin for the correlated flux pinning. As an evidence to support this discussion, the linearity of  $F_p$  to the magnetic field was more obvious at lower temperatures, which indicates that the flux pinning by the dislocation at the GBs is more effective at lower temperatures where the coherence length of the SmBCO is close to the size of the dislocation core ( $\sim 1$  nm) [24]. Let us estimate the field range in which the flux pinning by the dislocation core at the GB is effective. The maximum field is estimated to be 30 T for the dislocations at the GBs in the REBCO films at  $\theta = 5^\circ$  based on the dislocation distance of  $d_{\text{dis}} = a/\sin(\theta/2)$ , where  $a$  is the lattice constant of the REBCO matrix [13]. In order to prove this estimate, a further  $J_c$  measurement at a much higher field is desired.

In the BHO-doped SmBCO film with  $\theta = 0^\circ$  as shown in Fig. 2(c), peaks of  $F_p$  at  $B \sim 2$  T and saturations of  $F_p$  at  $B > 3$  T were observed at all the temperatures. The field for the  $F_p$  peaks corresponds to that of the end of the plateaus in the field dependence of the  $J_c$  as shown in Fig. 1(c). At magnetic fields below the peak fields, the  $F_p$  is proportional to the magnetic field. The peak of the  $F_p$  has been observed in the REBCO films with the straight and continuous nanorod APCs [15], [26]. This feature shows that the density of the BHO nanorods corresponds to the peak magnetic field of  $\sim 2$  T.

Finally, in the BHO-doped SmBCO film with  $\theta = 5^\circ$  as shown in Fig. 2(d), linear magnetic field dependences of the  $F_p$  with different slopes are observed in two magnetic field ranges. The peaks of  $F_p$  appear at  $B \sim 2$  T similar to the BHO-doped SmBCO films with  $\theta = 0^\circ$ . In addition, linear field dependences also appear at  $B > 4$  T at  $T < 20$  K similar to the undoped SmBCO film with  $\theta = 5^\circ$ . Therefore, the field dependence of the  $F_p$  in the BHO-doped film with  $\theta = 5^\circ$  is explained by the combination of the flux pinning due to the dislocation at the GBs and by the BHO nanorods. The results indicate that the A-J vortex at the GB is pinned more strongly with the BHO doping. Two possibilities are considered for the enhanced flux pinning of the A-J vortices. One is that the A-J vortex is directly pinned by the BHO nanorod grown at GB. The other is the A-J vortex is indirectly pinned by the interaction with the pinned vortices in the SmBCO grains with the BHO nanorods. Further study is needed to clarify which origin is valid.

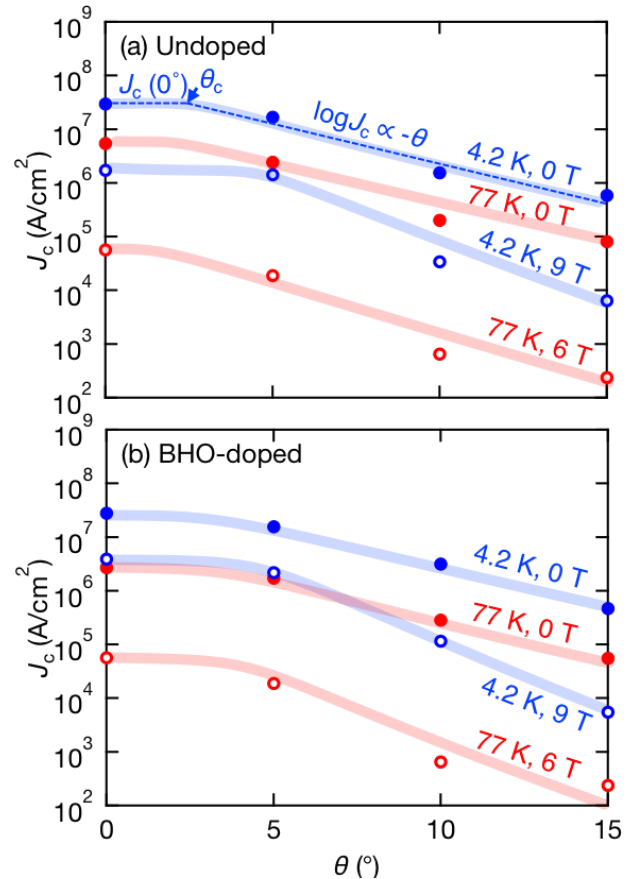


Fig. 3. Misorientation angle  $\theta$  dependence of  $J_c^{\text{GB}}$  at conditions of  $(T, B) = (4.2 \text{ K}, 0 \text{ T}), (4.2 \text{ K}, 9 \text{ T}), (77 \text{ K}, 0 \text{ T}),$  and  $(77 \text{ K}, 6 \text{ T})$  in (a) the undoped and (b) the BHO-doped SmBCO films.

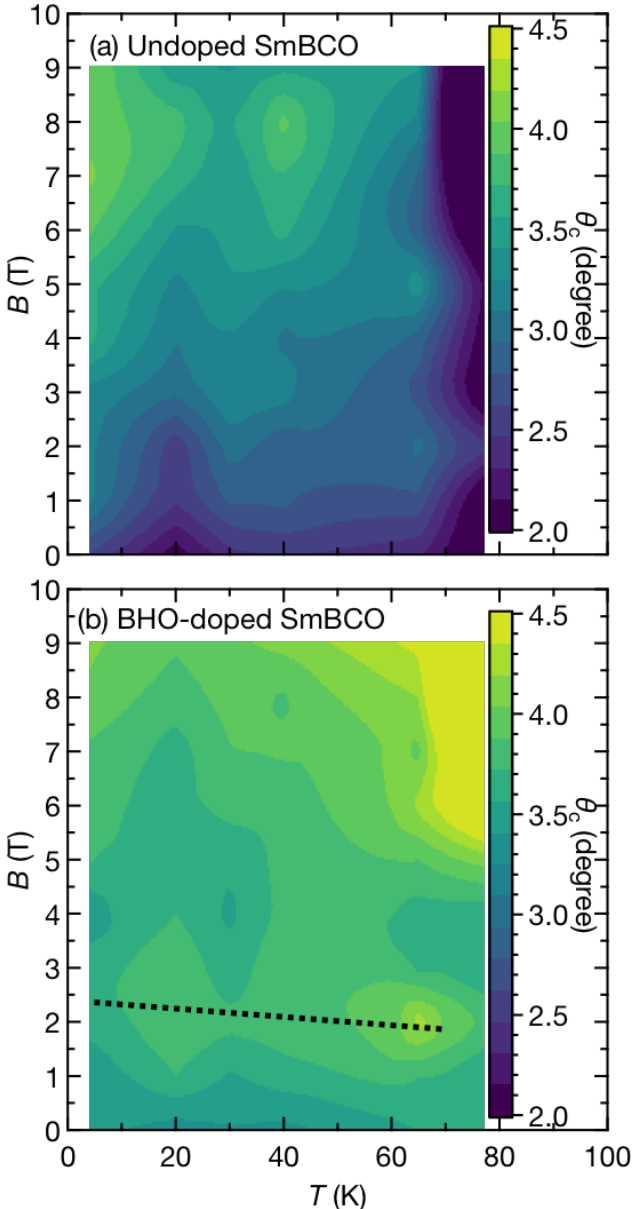


Fig. 4. Mappings of the critical misorientation angle  $\theta_c$  for magnetic fields and temperatures in (a) undoped and (b) BHO-doped SmBCO films.

### C. Critical misorientation angle

Fig. 3 shows  $\theta$  dependences of the  $J_c^{\text{GB}}$  in the undoped and the BHO-doped SmBCO films at conditions of  $(T, B) = (4.2 \text{ K}, 0 \text{ T}), (4.2 \text{ K}, 9 \text{ T}), (77 \text{ K}, 0 \text{ T}),$  and  $(77 \text{ K}, 6 \text{ T})$ . For all the conditions, the  $J_c^{\text{GB}}$  monotonically decreases with increasing  $\theta$ . According to the earlier study [15], the  $J_c^{\text{GB}}$  starts to decrease from a certain  $\theta$  which is called as the critical misorientation angle  $\theta_c$ . In this study, we defined the  $\theta_c$  as a crossover angle between the constant  $J_c^{\text{GB}}$  at low-angle GBs and the exponential decrease of the  $J_c^{\text{GB}}$  at high-angle GBs. The  $\theta_c$  is an important parameter to describe the allowance of the misorientation, and the larger  $\theta_c$  is preferable for the application. The  $\theta_c$  is estimated as follows. Draw a line with a constant  $J_c$  from  $\theta = 0^\circ$  as shown in Fig. 3(a). Then, a decay of  $J_c^{\text{GB}}$  for  $\theta > 0^\circ$  is fitted with an

exponential function. Finally, the  $\theta_c$  is estimated as a crossing  $\theta$  for both the lines.  $B$  and  $T$  dependences of the  $\theta_c$  is discussed in the following paragraphs. Fig. 4 shows the mapping of the  $\theta_c$  as a function of  $B$  and  $T$  for the undoped and the BHO-doped films. The mappings are colored in the same color scale. Overall, the  $\theta_c$  was higher for the BHO-doped films as  $3.2\text{-}4.4^\circ$  than that for the undoped films as  $2.0\text{-}4.0^\circ$  for a broad range of  $B$  and  $T$ . A region with the highly enhanced  $\theta_c$  was observed at  $T > 65 \text{ K}$  and  $B > 7 \text{ T}$ . We do not go into detail of this region because it is close to the irreversibility line of the SmBCO films. At a low  $T < 20 \text{ K}$  and a high  $B > 6 \text{ T}$ , the  $\theta_c$  is  $\sim 4^\circ$  regardless of the BHO doping. This common behavior is explained by the flux pinning by the dislocation at the GB because the correlated flux pinning by the dislocation is effective at low temperatures. Finally, in the BHO-doped films, the  $\theta_c$  shows a ridge at  $2\text{-}2.5 \text{ T}$  for wide  $T$  range as shown as a dotted line in Fig. 4(b). This field corresponds to the end field of the plateau of the  $J_c$  as shown in Fig. 1(c) and the peak field of the  $F_p$  as shown in Fig. 2(c) and 2(d). The pinning efficiency for the correlated pinning center is maximized in a magnetic field called a matching field where the density of vortices is equal to that of the pinning centers [23]. According to the previous study [21], the enhancement of  $J_c^{\text{GB}}$  is maximum at the matching field for the BHO-doped SmBCO films. Therefore, the ridge of the  $\theta_c$  in the BHO-doped SmBCO films in this study is due to the enhanced  $J_c^{\text{GB}}$  at the matching field for the BHO nanorod APCs. Note that the enhancement of the  $J_c^{\text{GB}}$  by the BHO doping is slight only for  $\theta = 15^\circ$ . It is possibly because the A-J vortex at the low-angle GBs is pinned by the APCs but the Josephson vortex at the high-angle GB is not. This result suggests that the  $\theta_c$  can be further improved by optimizing the flux pinning of the A-J vortices at the GBs such as changing the diameter of the nanorod APCs.

## IV. CONCLUSION

In this study, the low-temperature and the in-field superconducting properties at the GBs in the BHO-doped SmBCO bicrystalline films were investigated. As results, the  $J_c$ s at the low-angle GB were improved by the BHO doping at a broad ranges of temperatures and magnetic fields. The  $\theta_c$  in the SmBCO films were improved especially at a field around the matching field. This result suggests that the BHO doping into the SmBCO film is practical for fabrication of the coated conductors in terms of that the BMO APC doping makes  $J_c^{\text{GB}}$  less susceptible to the degree of orientation of the buffer layer on the substrate.

## REFERENCES

- [1] W. D. Markiewicz, D. C. Larbalestier, H. W. Weijers, A. J. Voran, W. R. Sheppard, J. Jaroszynski, A. Xu, J. Lu, A. V. Gavrilin, and P. D. Noyes, "Design of a Superconducting 32 T Magnet with REBCO High Field Coils", IEEE Trans. Appl. Supercond., vol. 22, no. 3, pp. 4300704–4300704, Jun. 2012.
- [2] G. A. Kirby, J. Nugteren, A. Ballarino, L. Bottura, N. Chouika, S. Clement, V. Datskov, L. Fajardo, J. Fleiter, R. Gauthier, L. Gentini, L. Lambert, M. Lopes, J. C. Perez, G. de Rijk, A. Rijllart, L. Rossi, H. ten Kate, M. Durante, P. Fazilleau, C. Lorin, E. Haro, A.

- Stenvall, S. Caspi, M. Marchevsky, W. Goldacker, and A. Kario, "Accelerator-Quality HTS Dipole Magnet Demonstrator Designs for the EuCARD-2 5-T 40-mm Clear Aperture Magnet", *IEEE Trans. Appl. Supercond.*, vol. 25, no. 3, p. 4000805, 2015.
- [3] K. Matsumoto and P. Mele, "Artificial pinning center technology to enhance vortex pinning in YBCO coated conductors", *Supercond. Sci. Technol.*, vol. 23, no. 1, p. 014001, Dec. 2009.
- [4] Y. Iijima, N. Tanabe, O. Kohno, and Y. Ikeno, "In-plane aligned  $\text{YBa}_2\text{Cu}_3\text{O}_{7-x}$  thin films deposited on polycrystalline metallic substrates", *Appl. Phys. Lett.*, vol. 60, no. 6, pp. 769–771, Jun. 1998.
- [5] B. Maiorov, S. A. Baily, H. Zhou, O. Ugurlu, J. A. Kennison, P. C. Dowden, T. G. Holesinger, S. R. Foltyn, and L. Civale, "Synergistic combination of different types of defect to optimize pinning landscape using  $\text{BaZrO}_3$ -doped  $\text{YBa}_2\text{Cu}_3\text{O}_7$ ", *Nat Mater.*, vol. 8, no. 5, p. 398, Apr. 2009.
- [6] P. Mele, K. Matsumoto, T. Horide, A. Ichinose, M. Mukaida, Y. Yoshida, S. Horii, and R. Kita, "Ultra-high flux pinning properties of  $\text{BaMO}_3$ -doped  $\text{YBa}_2\text{Cu}_3\text{O}_{7-x}$  thin films ( $M = \text{Zr}, \text{Sn}$ )", *Supercond. Sci. Technol.*, vol. 21, no. 3, pp. 032002–032006, Mar. 2008.
- [7] J. L. MacManus-Driscoll, S. R. Foltyn, Q. X. Jia, H. Wang, A. Serquis, L. Civale, B. Maiorov, M. E. Hawley, M. P. Maley, and D. E. Peterson, "Strongly enhanced current densities in superconducting coated conductors of  $\text{YBa}_2\text{Cu}_3\text{O}_{7-x} + \text{BaZrO}_3$ ", *Nat. Mater.*, vol. 3, no. 7, pp. 439–443, May 2004.
- [8] H. Tobita, K. Notoh, K. Higashikawa, M. Inoue, T. Kiss, T. Kato, T. Hirayama, M. Yoshizumi, T. Izumi, and Y. Shiohara, "Fabrication of  $\text{BaHfO}_3$  doped  $\text{GdBa}_2\text{Cu}_3\text{O}_{7-\delta}$  coated conductors with the high  $J_c$  of 85 A/cm-w under 3 T at liquid nitrogen temperature (77 K)", *Supercond. Sci. Technol.*, vol. 25, no. 6, p. 062002, May 2012.
- [9] Y. Tsuchiya, S. Miura, S. Awaji, Y. Ichino, K. Matsumoto, T. Izumi, K. Watanabe, and Y. Yoshida, "Flux pinning landscape up to 25 T in  $\text{SmBa}_2\text{Cu}_3\text{O}_y$  films with  $\text{BaHfO}_3$  nanorods fabricated by low-temperature growth technique", *Supercond. Sci. Technol.*, vol. 30, no. 10, p. 104004, Sep. 2017.
- [10] S. Miura, Y. Yoshida, Y. Tsuchiya, Y. Ichino, S. Awaji, A. Ichinose, K. Matsumoto, A. IBI, T. Izumi, and M. Iwakuma, "Strongly enhanced irreversibility field and flux pinning force density in  $\text{SmBa}_2\text{Cu}_3\text{O}_y$ -coated conductors with well-aligned  $\text{BaHfO}_3$  nanorods", *Appl. Phys. Express*, vol. 10, no. 10, pp. 103101–4, Sep. 2017.
- [11] D. Dimos, P. Chaudhari, J. Mannhart, and F. K. LeGoues, "Orientation Dependence of Grain-Boundary Critical Currents in  $\text{YBa}_2\text{Cu}_3\text{O}_{7-\delta}$  Bicrystals", *Phys. Rev. Lett.*, vol. 61, no. 2, pp. 219–222, Jul. 1988.
- [12] H. Hilgenkamp and J. Mannhart, "Grain Boundaries and Other Interfaces in Cuprate High- $T_c$  Superconductors", in *High- $T_c$  Superconductors and Related Materials*, no. 26, Dordrecht: Springer, Dordrecht, 2001, pp. 519–528.
- [13] D. Larbalestier, A. Gurevich, D. M. Feldmann, and A. Polyanskii, "High- $T_c$  superconducting materials for electric power applications", *Nature*, vol. 414, no. 6861, pp. 368–377, 2001.
- [14] J. H. Durrell and N. A. Rutter, "Importance of low-angle grain boundaries in  $\text{YBa}_2\text{Cu}_3\text{O}_{7-\delta}$  coated conductors", *Supercond. Sci. Technol.*, vol. 22, no. 1, pp. 013001–18, Nov. 2008.
- [15] A. Gurevich and E. A. Pashitskii, "Current transport through low-angle grain boundaries in high-temperature superconductors", *Phys. Rev. B*, vol. 57, no. 21, pp. 13878–13893, Jun. 1998.
- [16] D. T. Verebelyi, D. K. Christen, R. Feenstra, C. Cantoni, A. Goyal, D. F. Lee, M. Paranthaman, P. N. Arendt, R. F. DePaula, J. R. Groves, and C. Prouteau, "Low angle grain boundary transport in  $\text{YBa}_2\text{Cu}_3\text{O}_{7-\delta}$  coated conductors", *Appl. Phys. Lett.*, vol. 76, no. 13, pp. 1755–1757, Mar. 2000.
- [17] T. Horide, K. Matsumoto, Y. Yoshida, M. Mukaida, A. Ichinose, and S. Horii, "Tilt angle dependences of vortex structure and critical current density at low-angle grain boundaries in  $\text{YBa}_2\text{Cu}_3\text{O}_{7-x}$  films", *Phys. Rev. B*, vol. 77, no. 13, p. 132502, Apr. 2008.
- [18] T. Horide, K. Matsumoto, Y. Yoshida, M. Mukaida, A. Ichinose, and S. Horii, "The limitation mechanism of  $J_c$ - $\theta$  characteristics in  $\text{YBa}_2\text{Cu}_3\text{O}_{7-x}$  thin film with a single low angle grain boundary", *Physica C*, vol. 463, pp. 678–681, Oct. 2007.
- [19] A. Gurevich, M. S. Rzchowski, G. Daniels, S. Patnaik, B. M. Hinaus, F. Carillo, F. Tafuri, and D. C. Larbalestier, "Flux Flow of Abrikosov-Josephson Vortices along Grain Boundaries in High-Temperature Superconductors", *Phys. Rev. Lett.*, vol. 88, no. 9, pp. 969–4, Feb. 2002.
- [20] T. Horide, K. Matsumoto, Y. Yoshida, M. Mukaida, A. Ichinose, and S. Horii, "Combined effect of a single grain boundary and artificial pinning centers on the critical current density in a  $\text{YBa}_2\text{Cu}_3\text{O}_{7-\delta}$  thin film", *Appl. Phys. Lett.*, vol. 89, no. 17, pp. 172505–4, Oct. 2006.
- [21] A. Tsuruta, Y. Yoshida, A. Ichinose, S. Watanabe, T. Horide, K. Matsumoto, and S. Awaji, "Effect of  $\text{BaHfO}_3$  introduction on the transport current at the grain boundaries in  $\text{SmBa}_2\text{Cu}_3\text{O}_y$  films", *Appl. Phys. Express*, vol. 8, no. 3, p. 033101, Feb. 2015.
- [22] S. Miura, Y. Yoshida, Y. Ichino, A. Tsuruta, K. Matsumoto, A. Ichinose, and S. Awaji, "Flux pinning properties and microstructures of a  $\text{SmBa}_2\text{Cu}_3\text{O}_y$  film with high number density of  $\text{BaHfO}_3$  nanorods deposited by using low-temperature growth technique", *Jpn. J. Appl. Phys.*, vol. 53, no. 9, p. 090304, Aug. 2014.
- [23] G. Blatter, V. B. Geshkenbein, A. I. Larkin, and V. M. Vinokur, "Vortices in high-temperature superconductors", *Rev. Mod. Phys.*, vol. 66, no. 4, pp. 1125–1388, Oct. 1994.
- [24] A. Diaz, L. Mechin, P. Berghuis, and J. E. Evetts, "Evidence for Vortex Pinning by Dislocations in  $\text{YBa}_2\text{Cu}_3\text{O}_{7-\delta}$  Low-Angle Grain Boundaries", *Phys. Rev. Lett.*, vol. 80, no. 17, pp. 3855–3858, Apr. 1998.
- [25] S. Awaji, Y. Yoshida, T. Suzuki, K. Watanabe, K. Hikawa, and T. Izumi, "High-performance irreversibility field and flux pinning force density in  $\text{BaHfO}_3$ -doped  $\text{GdBa}_2\text{Cu}_3\text{O}_y$  tape prepared by pulsed laser deposition", *Appl. Phys. Express*, vol. 8, no. 2, p. 023101, Jan. 2015.
- [26] S. Miura, Y. Yoshida, Y. Ichino, Q. Xu, K. Matsumoto, A. Ichinose, and S. Awaji, "Improvement in  $J_c$  performance below liquid nitrogen temperature for  $\text{SmBa}_2\text{Cu}_3\text{O}_y$  superconducting films with  $\text{BaHfO}_3$  nano-rods controlled by low-temperature growth", *APL Mater.*, vol. 4, no. 1, pp. 016102–016109, Jan. 2016.